TEMPERATURE MODEL FOR HIGHLY TRANSIENT SHALLOW STREAMS

By Kyung Sub Kim[1] and Steven C. Chapra,[2] Associate Member, ASCE

ABSTRACT: The development and application of a one-dimensional heat transport model in highly transient streams governed by unsteady flow is described here. The resultant framework consists of two modules called the hydrodynamic and heat transport modules. In the hydrodynamic module, the hydraulic variables such as flow depth and velocity are simulated. Based on this information, the heat transport module is executed to calculate temperatures. A new approach—coupling heat transport in the surface water and diffusion in the sediment zone—is developed and applied for this module. In this approach, an interaction term accounts for the flux of heat energy between the water and sediments, which affects the distribution of water temperature in clear and shallow streams. Implicit finite difference methods called the Preissmann four-point and the Crank-Nicolson schemes are used to solve each module. Application of this framework demonstrates that the model effectively simulates the hydraulic variables and temperatures.

INTRODUCTION

At present, there are no general frameworks available to simulate the water quality of the small, highly transient streams found in the western United States. Consequently, because the proper modeling tools are unavailable, the management of small streams is severely hampered. This is true for conventional water-quality problems such as dissolved oxygen as well as more recent concerns such as ammonia toxicity and heavy metals contamination. To form the basis for subsequent integration of biological and chemical mechanisms, this paper deals with the two components of the physical environment that bear on the transport and fate of contaminants: hydrodynamics and heat.

The temperature of a water body is of particular significance for two reasons. First, by changing the ambient water temperature, excess heat can affect the aquatic ecosystem through direct lethal effects and chronic long-term effects on plants or animals. For example, the maximum desirable water temperature in a creek for salmon spawning habitat is approximately 13°C and for adult survival it is 24°C. Second, temperature influences all chemical and biological reactions. A general rule of thumb is that the rate will approximately double for a temperature rise of 10°C. Because of its large influence on many facets of the ecosystem, water temperature is clearly an important water-quality parameter. The accuracy of any water-quality model is sensitive to the results of the heat transport modeling it depends on.

The mathematical modeling of the transport and fate of heat in natural waters has been the subject of extensive study. Edinger et al. (1974) provide an excellent and comprehensive report of this research. Thomann and Mueller (1987) have summarized the fundamental approach as it relates to water-quality modeling. Most of this work has been oriented toward evaluating cooling water discharge and has dealt with systems such as large cooling ponds and rivers where heat exchange with the bottom sediments could be effectively neglected. In this paper, we focus on shallow systems where sediment-water heat exchange is significant. Generally, the standard models such as QUAL2E and **WASP4** are not applicable to the foregoing systems. A new treatment of heat transport which couples heat transport in the surface water and diffusion in the sediment zone is developed. The flux of heat energy between the water and sediments is incorporated to deal with the foregoing closure relations. We are particularly interested in the diurnal temperature variations of shallow, turbulent streams that are commonly found in upland regions. Although these systems are sometimes subjected to anthropogenic heat loads, their response to natural forcing functions is also of interest. Physical modification, such as channelization and riparian zone denudation, can have a pronounced effect on their thermal regimes. Mathematical models could prove useful in the evaluation of these modifications. In addition, diurnal temperature variations are relevant to the modeling of the fate of pollutants for such systems and the aquatic ecosystems.

The proposed models are applied using the data from Boulder Creek, Colorado and demonstrates that the model formulation contains sufficient realism to adequately simulate the physical environment of small, transient streams.

HYDRODYNAMIC MODULE

Existing water-quality models are based on an assumption of hydraulic steady state for large streams or rivers. Whenever the flow changes with time, as may happen in small streams found in the western United States, it becomes necessary to pay greater attention to a temporal description of the flow regime and its effect on the transport and mixing of quality constituents. Although the hydrodynamics of small transient streams are well understood, realistic flow models have never been adequately coupled with water-quality constituents. Because everything else in the framework will be strongly dependent on hydrodynamics, the first step in this paper is to develop the hydrodynamic module.

Strictly speaking, to simulate heat transport in a surface water system, the hydrodynamic module should be coupled with the heat transport module because the variations of water temperature change the density of water and affect the transport of constituents. An equation of state relating water density to temperature should be used. However, coupling the solutions is not practical in real environmental systems, because the time scale of the flow and transport processes is quite large.

To obtain a more efficient algorithm, we will neglect the density of water, which is only a relating term between the hydrodynamic and heat transport equations. Another reason to neglect this term is the degree of change is very small over large temperature variations. This approach has been successful in the modeling of channel networks (Cunge et al. 1980; Gromiec et al. 1983; Hauser 1991).

[1]Prof., Anseong Nat. Univ., 67 Seogjeong-ri Anseong-eub Anseong-gun Kyeong-gi-do, Korea; formerly, Res. Engr., Aquatic Envir. Sci., 350 S. 39th St., Boulder, CO 80303.

[2]Prof., Ctr. for Advanced Decision Support for Water and Envir. Sys., (CAD-SWES), Civ., Envir., and Arch. Engrg., Univ. of Colorado, Campus Box 428, Boulder, CO 80309-0428.

Note. Discussion open until June 1, 1997. To extend the closing date one month, a written request must be filed with the ASCE Manager of Journals. The manuscript for this paper was submitted for review and possible publication on July 1, 1994. This paper is part of the ***Journal of Hydraulic Engineering,*** Vol. 123, No. 1, January, 1997. ©ASCE, ISSN 0733-9429/97/0001-0030–0040/$4.00 + $.50 per page. Paper No. 8784.

Governing Equations

One-dimensional unsteady flow in streams, assuming that the density is constant, can be described by two dependent variables at any given stream cross section. These dependent variables define the state of the fluid motion along the water course and time, i.e., as a function of two independent variables, x for space and t for time. Amein and Chu (1975) noted that the flow rate Q, rather than the mean velocity u, is the preferred dependent variable in the governing equations because Q is, in general, a much smoother function of space and time.

Continuity equation

$$\frac{\partial A}{\partial t} + \frac{\partial Q}{\partial x} = q \tag{1}$$

where Q = flow rate (m^3s^{-1}); A = area of flow cross section ($b \times h$) (m^2); h = depth of flow (m); b = stream width (m); q = lateral inflow (m^2s^{-1}); t = time (s); and x = distance along the stream (m).

Momentum equation

$$\frac{\partial Q}{\partial t} + \frac{\partial}{\partial x}\left(\beta \frac{Q^2}{A}\right) + gA\frac{\partial h}{\partial x} + gA\frac{\partial z}{\partial x} + gAS_f - qu' = 0 \tag{2}$$

where g = acceleration due to gravity (ms^{-2}); z = bed elevation (m); β = momentum correction factor; u' = x-component average velocity of lateral inflows q (m^2s^{-1}); and S_f = energy slope.

In this module, two different hydrodynamic representations can be selected: one is dynamic and the other kinematic. Kinematic flow is described in the following model application section.

The Preissmann four-point implicit finite difference method is selected to get unconditionally stable solutions. The salient features of this method are found in Cunge et al. (1980) and Lyn and Goodwin (1987). This method used to express the va[illegible]nd partial derivatives of a function $f(x, t)$ within a four-po[illegible]d formed by the intersections of the space lines x_j and x_{j+1} [illegible] the time lines t^n and t^{n+1} are given by

$$\frac{\partial f}{\partial t} \approx \frac{1}{2}\left(\frac{f_{j+1}^{n+1} - f_{j+1}^{n}}{\Delta t} + \frac{f_j^{n+1} - f_j^n}{\Delta t}\right) \tag{3}$$

$$\frac{\partial f}{\partial x} \approx \frac{\theta}{\Delta x}(f_{j+1}^{n+1} - f_j^{n+1}) + \frac{1-\theta}{\Delta x}(f_{j+1}^n - f_j^n) \tag{4}$$

$$f \approx \frac{\theta}{2}(f_{j+1}^{n+1} + f_j^{n+1}) + \frac{1-\theta}{2}(f_{j+1}^n + f_j^n) \tag{5}$$

where θ = weighting factor $0.5 \le \theta \le 1$; Δx = step of space (m); and Δt = step of time (s). When $\theta = 0.5$ is used, this method reduces to a centered difference which is second-order accuracy in both space and time. When $\theta = 1$, a fully implicit method is formed.

Because the governing momentum equation has a nonlinear term, the Newton-Raphson method is adopted to solve the given equation (Chapra and Canale 1988; Chen and Simons 1975). The significant feature of the hydrodynamic equations is that in most cases the first iteration is so good, that there is no need for further iterations (Cunge et al. 1980). The solution benefits from the quadratic convergence characteristics of the Newton-Raphson method. The assemblage matrix of all stream reaches is obtained substituting (3)–(5) into the governing flow equations. This matrix is expressed as

$$\mathbf{A} \cdot \mathbf{X} = \mathbf{R} \tag{6}$$

where $\mathbf{A}$ = coefficient matrix; $\mathbf{X}$ = vector representing the unknown hydraulic variables; and $\mathbf{R}$ = forcing function vector aggregating the known values. With the addition of two boundary conditions the system can be solved. From the characteristics of the governing equations, it is well known that in subcritical flow the inflow boundary condition and outflow boundary condition are needed, but in supercritical flow two inflow conditions are required. A detailed account of the foregoing numerical formulation is found in Kim (1993).

As given by (6), application of the Preissmann four-point method results in the formation of a linear system of algebraic equations. If the matrix $\mathbf{A}$ has a bandwidth of three, (6) may be solved for $\mathbf{X}$ using the Thomas algorithm (Chapra and Canale 1988). This approach exploits the tridiagonal structure of $\mathbf{A}$ by eliminating useless operations on zero elements. The double sweep method, which is similar to the Thomas algorithm, can also be used (Liggett and Cunge 1975; Lai 1986).

HEAT TRANSPORT MODULE

Applying the principle of conservation of thermal energy to a one-dimensional vertically well-mixed open channel or stream, the conservative form of the transport equation becomes

$$\frac{\partial T}{\partial t} + u\frac{\partial T}{\partial x} = \frac{\partial}{\partial x}\left(D\frac{\partial T}{\partial x}\right) + \frac{q}{A}(T_L - T) + \frac{H_T w}{C_w \rho_w A} \tag{7}$$

where T = cross-sectional average water temperature (°C); T_L = water temperature in lateral inflow (°C); D = longitudinal dispersion coefficient (m^2s^{-1}); H_T = surface flux of thermal energy ($J\ m^{-2}s^{-1}$); w = top width of the channel (m); C_w = specific heat of water ($J\ kg^{-1}\ °C^{-1}$); and ρ_w = density of water ($kg\ m^{-3}$). Edinger et al. (1974), Eagleson (1970), and Thomann and Mueller (1987) provide a full and detailed treatment of heat exchange at the air-water interface.

For most deep channels, the thermal flux through the channel bottom is insignificant. However, as reported by Jobson (1980) and Jobson and Keefer (1979), the bed conduction term may be significant in determining the diurnal or annual variation of temperature in water bodies with depths of 3 m or less. To consider the bed conduction, the following term $(H_B p)/(C_w \rho_w A)$ should be added on the right-hand side of (7), where p is the wetted perimeter of the channel (m) and H_B is the flux of thermal energy due to temperature differential between the water and bed.

Surface Flux of Thermal Energy

An overview of the features to be included in the surface flux of thermal energy H_T is described. To develop a general module, it will be necessary to create an adaptable procedure by which various problems are defined. Measured data and empirical equations are used for each individual term of H_T. An interpolation or linearization technique can be applied to increase module flexibility and economize computational time. The former technique is applied to estimate intermediate values between precise data points and the latter technique is used to linearize a nonlinear term.

Shortwave Radiation (H_s and H_{sr})

Incoming solar radiation H_s can be measured directly. The reflection of solar radiation H_{sr} depends on the sun's altitude, cloud cover, and water conditions. Fresnel's reflectivity law provides an estimate of the percentage reflection H_{sr}/H_s (Neumann and Pierson 1966) without considering the cloud cover and water conditions.

To obtain H_{sr} from real data at each solar altitude $\tilde{\beta}$ point, the total region of $\tilde{\beta}$ (0° to 90°) is divided into three subregions with similar characteristics (Kim 1993). When $\tilde{\beta}$ is less than 60°, a six-order polynomial interpolation method is used

$$H_{sr} = (284.2 - 286.793x + 132.161x^2 - 34.3354x^3 + 5.17431x^4 - 0.42125x^5 + 0.0143056x^6)H_s/100 \quad (8)$$

where $x = 1 + \tilde{\beta}/10$. When $\tilde{\beta}$ is greater than 60° and less than 80°, the constant ratio of H_{sr}/H_s is used

$$H_{sr} = 2.1H_s/100 \quad (9)$$

and $\tilde{\beta}$ is greater than 80°, then the linear decrease of the ratio of H_{sr}/H_s is used

$$H_{sr} = (-0.01\tilde{\beta} + 2.9)H_s/100 \quad (10)$$

Long-Wave Radiation (H_a and H_{ar})

The long-wave radiation H_a can be measured or estimated from the following (Thomann and Mueller 1987):

$$H_a = \sigma(T_a + 273)^4(A' + 0.031\sqrt{e_a}) \quad (11)$$

where σ = Stefan-Boltzmann constant (J $m^{-2}s^{-1}$ $°K^{-4}$); T_a = air temperature (°C); e_a = air-vapor pressure (kg $m^{-1}s^{-2}$); and A' = coefficient related to air temperature (0.5–0.7). The reflected long-wave radiation H_{ar} is generally small, about 3% of the incoming long-wave radiation.

To obtain e_a, we have to know the relative humidity R'. Generally, dew-point temperature is measured along with other meteorological variables. The following relationship can be used to calculate the relative humidity:

$$R' = e^{[(T_d - T_a)/15.7945]} \quad (12)$$

where T_d = dew-point temperature (°C). A detailed account of (12) is found in Kim (1993).

Long-Wave Radiation (H_{br})

The long-wave radiation H_{br} emitted by the water follows the Stefan-Boltzmann law for a black body and is given by (Thomann and Mueller 1987)

$$H_{br} = \varepsilon\sigma(T + 273)^4 \quad (13)$$

where ε = emissivity of water. Because the variation of H_{br} appears linearly related to the change of water temperature, a linearization technique is adopted for efficiency. Dividing the region into three subregions and using the ε of 0.97, the equations in Table 1 are determined for each temperature subregion.

Conductive Heat Transfer (H_c)

The rate of conductive heat transfer H_c depends on the temperature difference between the water and the air as well as the wind speed over the water (Thomann and Mueller 1987)

$$H_c = c_1(19.0 + 0.95U_w^2)(T - T_a) \quad (14)$$

where c_1 = Bowen's coefficient (kg $m^{-1}s^{-2}$ $°C^{-1}$); and U_w = wind speed measured at a height of 7 m above the water (ms^{-1}); H_c is positive when the water temperature is greater than the air temperature.

TABLE 1. New Long-Wave Radiation Equations Emitted by Water

Temperature (°C) (1)	H_{br} (J $m^{-2}s^{-1}$) (2)	r^2 (3)
$-5 \le T \le 10$	$305.9054 + T \times 4.603116$	0.999503
$10 < T \le 25$	$297.89150 + T \times 5.1460046$	0.999553
$25 < T \le 40$	$275.8170 + T \times 6.275959$	0.999595

Note: r is the correlation coefficient.

TABLE 2. Saturated Vapor Pressure Equations

Temperature (°C) (1)	e_{sat} (kg $m^{-1}s^{-2}$) (2)
$T < 0$	$610.483 + T \times 37.7569$
$0 \le T < 5$	$610.483 + T \times 52.3690$
$5 \le T < 10$	$516.891 + T \times 71.0875$
$10 \le T < 15$	$273.444 + T \times 95.4322$
$15 \le T < 20$	$-193.717 + T \times 126.5763$
$20 \le T < 25$	$-979.786 + T \times 165.8797$
$25 \le T < 30$	$-2{,}211.018 + T \times 215.1290$
$30 \le T < 35$	$-4{,}037.268 + T \times 276.0040$
$35 \le T$	$-6{,}648.520 + T \times 350.6112$

Evaporation (H_e)

Edinger et al. (1974) have suggested the following formula to compute the rate of heat loss by evaporation H_e

$$H_e = (19.0 + 0.95U_w^2)(e_{sat} - e_a) \quad (15)$$

where e_{sat} = saturated vapor pressure of water (kg $m^{-1}s^{-2}$). Because e_{sat} is the function of water temperature T, e_{sat} can be related to T linearly to attain a more efficient algorithm in a similar fashion to the long-wave radiation H_{br}. Table 2 is developed to compute e_{sat} in a linear piecewise fashion for several subregions of water temperature.

Rain Falling (H_R)

The water temperature can be increased or decreased by accounting for rain falling in stream (Jobson and Keefer 1979)

$$H_R = C_w\rho_w I(T_w - T) \quad (16)$$

where I = rainfall rate (ms^{-1}); and T_w = wet-bulb air temperature (°C).

Net Solar Radiation Available for Warming Channel Bed (H_{nsr})

If a stream is shallow, the net solar radiation available for warming the channel bed, H_{nsr}, should be incorporated in this module. Measurements of solar radiation absorption with depth in a body of water that initially there is a region of rapid attenuation followed by an exponential variation (Dake and Harleman 1969; Babajimopoulos and Papadopoulos 1986). The H_{nsr} at any flow depth h is described by

$$H_{nsr} = (1 - A_b)(1 - \beta')e^{-\eta h}(H_s - H_{sr}) \quad (17)$$

where A_b = albedo of bed material; β' = fraction of solar radiation absorbed at the surface water; and η = extinction coefficient (m^{-1}).

The final expression of H_T can be written as

$$H_T = [(H_s - H_{sr} - H_{nsr}) + (H_a - H_{ar})] - (H_{br} \pm H_c \pm H_e \pm H_R) \quad (18)$$

The first group of terms in brackets on the right-hand side of (18) is independent of the water temperature and the second group of terms depends in various ways on the water temperature.

Bed Conduction

Jobson (1977, 1980) proposed the following method in which the heat flux into or out of the bed can be determined as a function of the history of the water temperature, with the bed assumed to be a homogeneous medium insulated on the lower face (bed) and with the upper face always having a temperature equal to that of the overlying water. A constant bed thickness exceeding the depth of temperature variations is

assumed to make the heat flux equations more convenient computationally.

In this paper, a new approach is proposed to solve the heat transport equation, including a new equation providing the temperature distribution in the sediment zone.

Proposed Process

The one-dimensional distribution of temperature in a sediment having homogeneous properties with depth can be formulated as

$$\frac{\partial T_s}{\partial t} = \alpha \frac{\partial^2 T_s}{\partial z^2} \tag{19}$$

where T_s = sediment temperature (°C); and α = thermal diffusivity of the sediment (m^2s^{-1}). Here, z equals zero at the sediment-water interface and decreases downward.

Given boundary conditions and initial conditions, (19) can be solved numerically for the time-variable distribution of temperature. Also, (19) can be solved analytically with the ideal boundary conditions such as $T_s = T = a \times \sin(\omega t) + T_m$ at $z = 0$ and $T_s = T_m$ at $z = \infty$, where T_m is the mean water temperature (°C); a is the amplitude; and ω is the angular frequency (rad s^{-1}). It is assumed that the water temperature is constant at any given cross section in a one-dimensional well-mixed channel and there is a deep sediment temperature subject to a sinusoidal diurnal variation. Initial conditions can be obtained at any time and applied for the proposed module that incorporates the following equation to account for a thermal energy flux at the sediment-water interface:

$$H_B + H_{nsr} = -k \frac{\partial T_s}{\partial z}\bigg|_{z=0} \tag{20}$$

where k = thermal conductivity (J $m^{-1}s^{-1}$ °C^{-1}). The foregoing analytical approach for an ideal case is found in Kim (1993).

The direction of thermal energy at $z = 0$ depends on the sign on the left-hand side of (20). If $H_B + H_{nsr}$ is positive, the thermal energy moves from water to sediment. As described in Kim (1993), if convective heat transfer at the sediment-water interface is comparable to heat conduction in the sediments, another approach should be considered. For turbulent and/or shallow water systems found in the western United States, (20) holds because the flux of thermal energy at the sediment-water interface would be limited by heat conduction in the sediments.

Governing Equations

The governing equations for the newly developed heat transport module are composed of three equations, i.e., (7), (19), and (20), with three unknown values T, T_s, and H_B. To account for the temperature variation in the sediment zone, (19) is used and (7) is used to simulate a heat transport in surface water systems. The governing equations are combined with the flux of heat energy at the sediment-water interface represented by (20). The numerical formulation of this module becomes a quasi, two-dimensional type along a stream distance and a sediment zone.

Crank-Nicolson Method

The Crank-Nicolson method is used for the numerical formulation of the governing equations. There are two main reasons to select this method. First, it is to provide compatibility with the spatial and temporal grid used for the implicit finite difference algorithm for the hydrodynamics. Second, this method, which has a property of second-order accuracy in both space and time, is a popular scheme applied to a parabolic-type equation.

The partial derivative in time and the first and second derivative in space can be determined at the midpoint by averaging the difference approximations at the beginning and at the end of the time increment

$$\frac{\partial f}{\partial t} \approx \frac{f_j^{n+1} - f_j^n}{\Delta t} \tag{21}$$

$$\frac{\partial f}{\partial x} \approx \frac{1}{2}\left(\frac{f_{j+1}^{n+1} - f_{j-1}^{n+1}}{2\Delta x} + \frac{f_{j+1}^n - f_{j-1}^n}{2\Delta x}\right) \tag{22}$$

$$\frac{\partial^2 f}{\partial x^2} \approx \frac{1}{2}\left[\frac{f_{j+1}^{n+1} - 2f_j^{n+1} + f_{j-1}^{n+1}}{(\Delta x)^2} + \frac{f_{j+1}^n - 2f_j^n + f_{j-1}^n}{(\Delta x)^2}\right] \tag{23}$$

$$f \approx \frac{1}{2}(f_j^{n+1} + f_j^n) \tag{24}$$

To assess the stability of a given numerical algorithm, Hoffman (1992) conducted von Neumann stability analysis, which gives the necessary and sufficient stability criteria in a straightforward and uncomplicated manner, for a linear convection-dispersion and a diffusion equation. From this analysis, it is known that the Crank-Nicolson method is consistent and unconditionally stable.

Numerical Formulations

Substituting (21)–(24) into (7), including H_B, and arranging gives the following expression for a generic segment from x_{j-1} to x_{j+1}:

$$\left(-\frac{1}{2}u_j^{n+1} - \frac{D_{j-1/2}^{n+1}}{\Delta x}\right)T_{j-1}^{n+1} + \left(2\frac{\Delta x}{\Delta t} + \frac{D_{j+1/2}^{n+1} + D_{j-1/2}^{n+1}}{\Delta x} + \Delta x\frac{q_j^{n+1}}{A_j^{n+1}}\right)$$
$$\cdot T_j^{n+1} + \left(\frac{1}{2}u_j^{n+1} - \frac{D_{j+1/2}^{n+1}}{\Delta x}\right)T_{j+1}^{n+1} = \left(\frac{1}{2}u_j^n + \frac{D_{j-1/2}^n}{\Delta x}\right)T_{j-1}^n$$
$$+ \left(2\frac{\Delta x}{\Delta t} - \frac{D_{j+1/2}^n + D_{j-1/2}^n}{\Delta x} - \Delta x\frac{q_j^n}{A_j^n}\right)T_j^n + \left(-\frac{1}{2}u_j^n + \frac{D_{j+1/2}^n}{\Delta x}\right)$$
$$\cdot T_{j+1}^n + \Delta x\left[\frac{q_j^n}{A_j^n}(T_L)_j^n + \frac{q_j^{n+1}}{A_j^{n+1}}(T_L)_j^{n+1}\right]$$
$$+ \frac{\Delta x}{C_w\rho_w}\left[\frac{(H_T + H_B + H_{nsr})_j^n}{h_j^n} + \frac{(H_T + H_B + H_{nsr})_j^{n+1}}{h_j^{n+1}}\right] \tag{25}$$

where $(H_T w)/(C_w\rho_w A) + (H_B p)/(C_w\rho_w A)$ is replaced by $(H_T + H_B)/(C_w\rho_w h)$ in shallow water systems. The left-hand side of (25) is related to the unknown water temperatures at the next time step and the right-hand side is given by the known variables and parameters, except for the last term. Substituting (21) and (23) into (19) gives

$$-\frac{\alpha_j^{n+1}}{\Delta z}T_{s,j-1}^{n+1} + \left(2\frac{\Delta x}{\Delta t} + \frac{\alpha_j^{n+1}}{\Delta z}\right)T_{s,j}^{n+1} - \frac{\alpha_j^{n+1}}{\Delta z}T_{s,j+1}^{n+1}$$
$$= \frac{\alpha_j^n}{\Delta z}T_{s,j-1}^n + \left(2\frac{\Delta x}{\Delta t} - \frac{\alpha_j^n}{\Delta z}\right)T_{s,j}^n + \frac{\alpha_j^n}{\Delta z}T_{s,j+1}^n \tag{26}$$

where Δz = space step into the sediment (m).

Before coupling (25) and (26), it is necessary to reexpress (25) for $H_B + H_{nsr}$. Also, some terms in the surface flux of thermal energy $(H_T)_j^{n+1}$ should be moved to the left-hand side of (25), because the terms of long-wave radiation H_{br} and evaporation H_e in $(H_T)_j^{n+1}$ is a function of water temperature T_j^{n+1}.

The interpolation technique is used for numerical formulation of (20). This approach stems from the assumption that the calculated values of sediment temperature are precise. The fifth-order polynomial interpolation with equal-sized segments gives, at the present and future time step

$$(H_B)^n_{j,z_1} + (H_{nsr})^n_j = k\left(\frac{137}{60\Delta z}T^n_{j,z_1} - \frac{5}{\Delta z}T^n_{j,z_2} + \frac{5}{\Delta z}T^n_{j,z_3} - \frac{10}{3\Delta z}T^n_{j,z_4} + \frac{5}{4\Delta z}T^n_{j,z_5} - \frac{1}{5\Delta z}T^n_{j,z_6}\right) \quad (27)$$

and

$$(H_B)^{n+1}_{j,z_1} + (H_{nsr})^{n+1}_j = k\left(\frac{137}{60\Delta z}T^{n+1}_{j,z_1} - \frac{5}{\Delta z}T^{n+1}_{j,z_2} + \frac{5}{\Delta z}T^{n+1}_{j,z_3} - \frac{10}{3\Delta z}T^{n+1}_{j,z_4} + \frac{5}{4\Delta z}T^{n+1}_{j,z_5} - \frac{1}{5\Delta z}T^{n+1}_{j,z_6}\right) \quad (28)$$

where the first subscript represents the calculation segments of the stream reach and the second subscript represents the depth of sediment. It is known that the sediment temperature T_{j,z_1} at the location z_1 is equal to the water temperature T_j. The derivation of (27) or (28) is found in Kim (1993).

Linking (25), (26), (27), and (28) yields a matrix form similar to that of (6). The right-hand side of (6) comes from the known values at the present time step such as the right-hand side of (25), (26), and (27). The elements in the matrix A are related to the coefficients of the left-hand side in (25) and (26) and the right-hand side in (28). The matrix form of (6) is a system of $NX \times NZ - 2$ equations for $NX \times NZ + NX$ unknowns in which NZ is the number of segments into the sediment.

The number of $NX + 2$ boundary conditions should be incorporated to solve the matrix. Two boundary conditions come from the points of inflow and outflow over the entire computational domain and other NX boundary conditions come from the deep sediment points. The penetration depth into the sediments is very important to apply boundary conditions in the sediment zone. If the sediment depth is selected to account for no temperature variation at that depth, the following expression holds:

$$k\left.\frac{dT}{dz}\right|_{z=L_2} = 0 \quad (29)$$

where L_2 = sediment depth. Thus, there are $NX \times NZ - 2$ equations for $NX \times NZ - 2$ unknowns in this system.

Testing of Numerical Algorithm

Numerical tests were conducted to assess the newly developed algorithm. The flux of thermal energy at the sediment-water interface and the temperature profile in the sediment zone calculated by this module were compared with analytical values when the ideal boundary condition is imposed at the sediment-water interface. The parameters shown in Table 3 are selected.

First, to know the behavior of the fifth-order polynomial interpolation approach for (20), the results of this approach were compared with a second-order polynomial, a third-order

TABLE 3. Parameters for Test

Parameter (1)	Value (2)
Amplitude of the water temperature a	1
Simulation period (hr)	24
Sediment depth L_2 (m)	0.6
Space step for sediment zone Δz (m)	0.02
Time step Δt (s)	30
Thermal diffusivity α (m^2s^{-1})—sand dry	0.0000003
Specific heat C_s (J kg^{-1} $°C^{-1}$)—sand dry	795.2
Density ρ_s (kg m^{-3})—sand dry	1,750
Albedo of bed material A_b	0.5
Fraction of solar radiation absorbed at surface water β'	0.4
Extinction coefficient η (m^{-1})	0.05

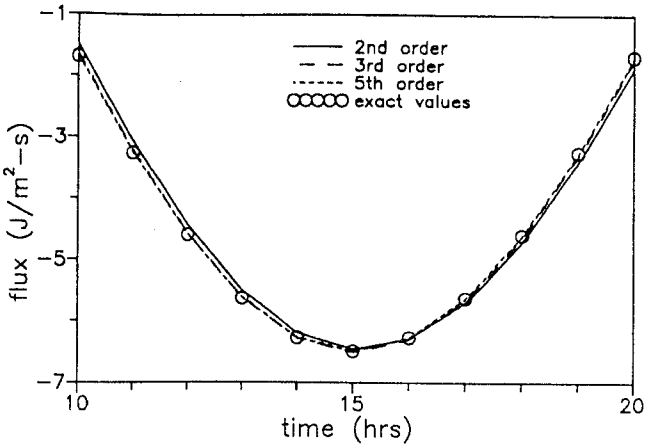

FIG. 1. Thermal Energy Flux at Sediment-Water Interface

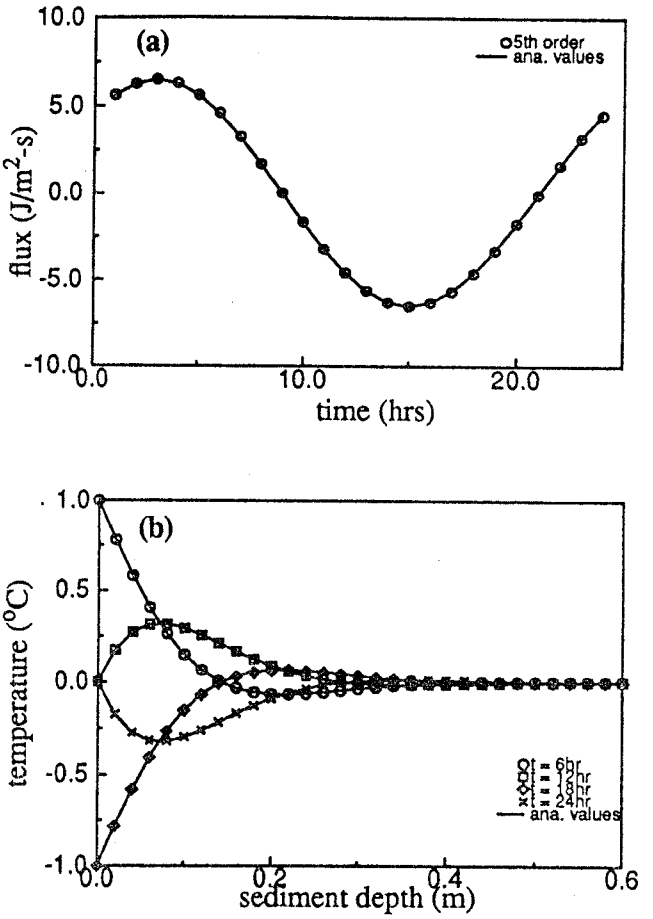

FIG. 2. Thermal Energy Flux at Sediment-Water Interface and Temperature Profile in Sediment Zone

polynomial, and the exact values in Fig. 1. The comparison indicates that the fifth-order approach more closely follows the analytical values.

Fig. 2 shows the thermal energy flux at the sediment-water interface and temperature profile in the sediment zone. From Fig. 2, we see that the heat transport module incorporating the sediment heat exchange term simulates precisely the flux of thermal energy and the distribution of temperature in the sediment zone.

MODEL APPLICATION

Boulder Creek Observations, 1987

A comprehensive 24-h synoptic survey was conducted on September 21 and 22, 1987. A complete description of the

survey can be found in Windell et al. (1988). The study area consists of an 13.7 km (8.5 mi) stretch of Boulder Creek from the Boulder Wastewater Treatment Plant (WWTP) to the confluence with Coal Creek. Sampling was conducted at several locations along the creek such as LB-0.1 (immediately upstream of Boulder WWTP), LB 0.0 (WWTP effluent), LB 0.4, LB 3.5, LB 5.6, and LB 8.5 (immediately upstream of the Boulder Creek/Coal Creek confluence). The numbers associated with each site represent the creek miles downstream from Boulder WWTP.

Solution Procedure

At the heart of a resultant framework is the idea of solving the hydrodynamic module and the heat transport module in two distinct steps. For a given time step, the hydrodynamic module is called to simulate the hydraulic variables. Then the heat transport module is called to calculate water temperature based on the foregoing information. After completing the heat transport step, this sequence is repeated until the end of the simulation period is reached.

Hydrodynamic Module

After reviewing the available data, first it was assumed that the study area could be divided into two reaches: mile points $-0.1-3.5$ and mile points 3.5 and 8.5. This division was based on the morphometry of Boulder Creek. There is also reason to believe that these two reaches have differences. For example, the lower reach has been subjected to much more channelization than the upper reach, which has a meandering nature. Also, the slopes of each reach, which are strongly related to travel time, are different. The second reach was divided into two subreaches to consider the difference of top width. Consequently, three reaches with a rectangular cross-sectional shape were adopted for Boulder Creek. The rectangular shape seems a reasonable compromise because the hydraulic radius is close to the water depth. Fig. 3 shows the network of Boulder Creek for the hydrodynamic and heat transport modules.

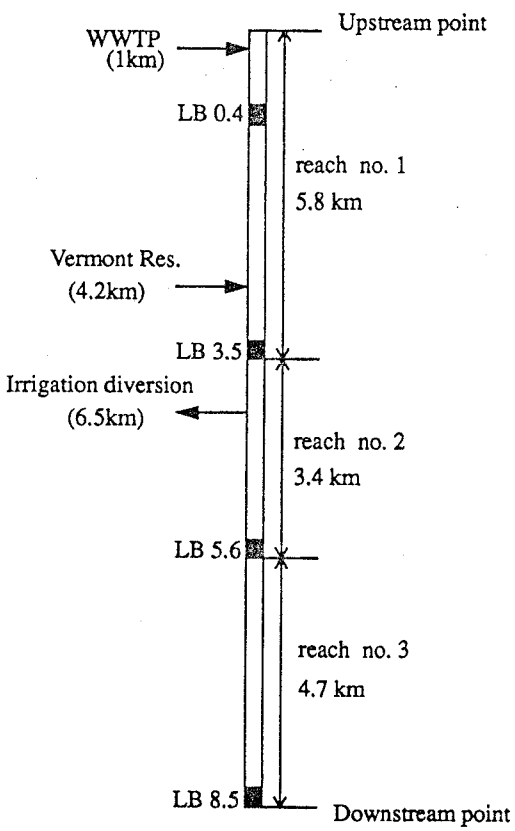

FIG. 3. Network of Boulder Creek

Sufficient data, such as the rating curve of discharge at the creek entrance point and flow depth at the creek exit point, are essential to run the unsteady flow equations. Based on the available Boulder Creek data set, simplified flow equations are applied. Another reason to apply simplified flow equations is that the terms of (2) have different relative importance in different flow situations.

Simplified Flow Equations—Kinematic Wave

Reformulating (2) after neglecting β and u' gives

$$\frac{1}{g}\frac{\partial u}{\partial t} + \frac{u}{g}\frac{\partial u}{\partial x} + \frac{\partial h}{\partial x} + \frac{\partial z}{\partial x} + S_f = 0 \tag{30}$$

From the measured values, we can assume that the flow velocity at LB 3.5 changes from 0.4 to 0.24 m/s in 6 h and that the value changes from 0.4 to 0.12 m/s along a distance of between LB 5.6 and LB 3.5 over 3.4 km. The variations of the flow velocity are larger than any other values in Boulder Creek. Then the first two terms of (30) are of the order of $1/9.8 \times 0.16/(3{,}600 \times 6) \approx 7.6 \times 10^{-7}$ and $0.4/9.8 \times 0.28/3{,}400 \approx 3.4 \times 10^{-6}$, respectively. The bottom slope of Boulder Creek is about $3-4 \times 10^{-3}$ while the friction slope is also of the order of 10^{-3}. Thus, the first and second terms on the left-hand side of (30) are rather small values and we can neglect these terms according to their relative importance in the Boulder Creek flow situation. After neglecting the inertia terms such as the local and advective accelerations, in channels with a sufficiently steep slope (Boulder Creek) and without backwater effects, we can also neglect the term $\partial h/\partial x$ as being small compared to $\partial z/\partial x$, which then reduces to the kinematic wave equation

$$Q = K(h)\sqrt{S_0} \tag{31}$$

where K = conveyance factor; and S_0 is the channel bottom slope ($= \partial z/\partial x$). If the Manning equation is used, K is equal to $AR^{2/3}/n$, where n is Manning's coefficient and R is the hydraulic radius (m).

Eq. (31) implies that $Q = Q(h)$ and $h = h(Q)$, i.e., that there is a single-valued relationship between the depth and the discharge. Consequently, the simplified flow governing equation is developed after substituting (31) into (1)

$$b\left(\frac{n}{b\sqrt{S_0}}\right)^{3/5}\frac{\partial Q^{3/5}}{\partial t} + \frac{\partial Q}{\partial x} = q \tag{32}$$

As long as the characteristics of (32) do not intersect, there is only one characteristic direction at each point of the (x, t) plane. Thus, the solution $Q(x, t)$ of (32) requires initial values $Q(x, 0)$ at each calculation point and one boundary condition $Q(0, t)$. The linearization technique is applied because (32) has a nonlinear term. A more detailed description of the kinematic wave model is found in Cunge et al. (1980) and Liggett and Cunge (1975).

Data for Hydrodynamic Module

Table 4 shows the parameters for the simplified flow equation represented by (32). From this table, the hydraulic char-

TABLE 4. Parameters for Hydrodynamic Module

Reach number (1)	Creek width (m) (2)	Lateral flow rate (m^2s^{-1}) (3)	Manning coefficient (4)	Creek slope (5)
1	13	0.0	0.1	0.003247
2	13.6	−0.00023	0.14	0.003788
3	11	0.0	0.13	0.003788

acteristic of Boulder Creek is assured, i.e., the measured flow depth is in the 0.2–0.6 m range. The lateral flow rate of each reach was estimated after calibration of the simulation results. The minus value of lateral flow means that water is withdrawn from the water body. The creek slope was obtained from 1: 24,000 scale topographic maps and the other parameters were estimated from the measured values. The Manning coefficient is relatively high due to steep creek slopes.

The flow rates of station LB-0.1 do not change much over a simulation period. Consequently, a constant value of 0.71 m^3s^{-1} was used as an inflow boundary condition. The initial values of flow rate were chosen from the measured values with the assumption that the values vary linearly with the creek distance between points of observation. The flow rates of the WWTP effluent were regressed from the measured values. A regression technique with sinusoidal functions was used, because the data has the property of a periodic shape over a simulation period.

Simulation Results

The simulation period starts at 4 a.m. on September 21, 1987 and ends at 4 a.m. on September 22, 1987. The module was run for two days, because the initial values of the flow rate were approximated from the measured values. The first 24-h period was used to eliminate any numerical transients created by the approximation of initial conditions, and the second 24-h period was used for comparison with field observations.

There are no measured flow rates for Vermont Reservoir and the irrigation diversion points. After initial calibration with the field observations, the flow rate of each point was estimated. Fig. 4 shows the measured and calculated values of flow rate with $\Delta t = 30$ s and $\Delta x = 100$ m. A sensitivity analysis of the importance of the time step indicated that no significant differences in the accuracy of the solution is obtained for a 30–120 s range (Kim 1993). The time step $\Delta t = 120$ s is used to run the heat transport module.

Heat Transport Module

Eq. (7), including bed conduction, is used without making any simplifying assumptions.

Dispersion Coefficient (D)

A considerable investigation of the dispersion coefficient has been made, because that is the most uncertain parameter. A variety of theoretical and empirical relationships have been proposed. In this paper, the dispersion coefficient is computed from the following equation (Bowie et al. 1985; Brown and Barnwell 1987; Jobson 1975; Jobson and Keefer 1979; Fischer et al. 1979), which is the most widely used one in the environmental engineering field

$$D = C_d R u_* \tag{33}$$

where C_d = dispersion constant; and u_* = shear velocity (ms^{-1}).

Generally, the dispersion constant ranges from about 6 for straight smooth channels to about 500 for some natural channels. Considering the geometry of Boulder Creek and the experimental measurements of dispersion coefficient in natural channels (Brown and Barnwell 1987), values in the 250–500 range seem a reasonable compromise. The proper value of the dispersion constant can be estimated from the parameter calibration of this module.

The shear velocity u_* is expressed

$$u_* = \sqrt{gRS_0} \tag{34}$$

The depth of a stream is always less than the channel width in natural streams. R can be approximated by h at large width to depth ratios. Substituting (34) into (33) and assuming $R \approx h$ gives

$$D = C_d(gS_0)^{1/2}h^{3/2} \tag{35}$$

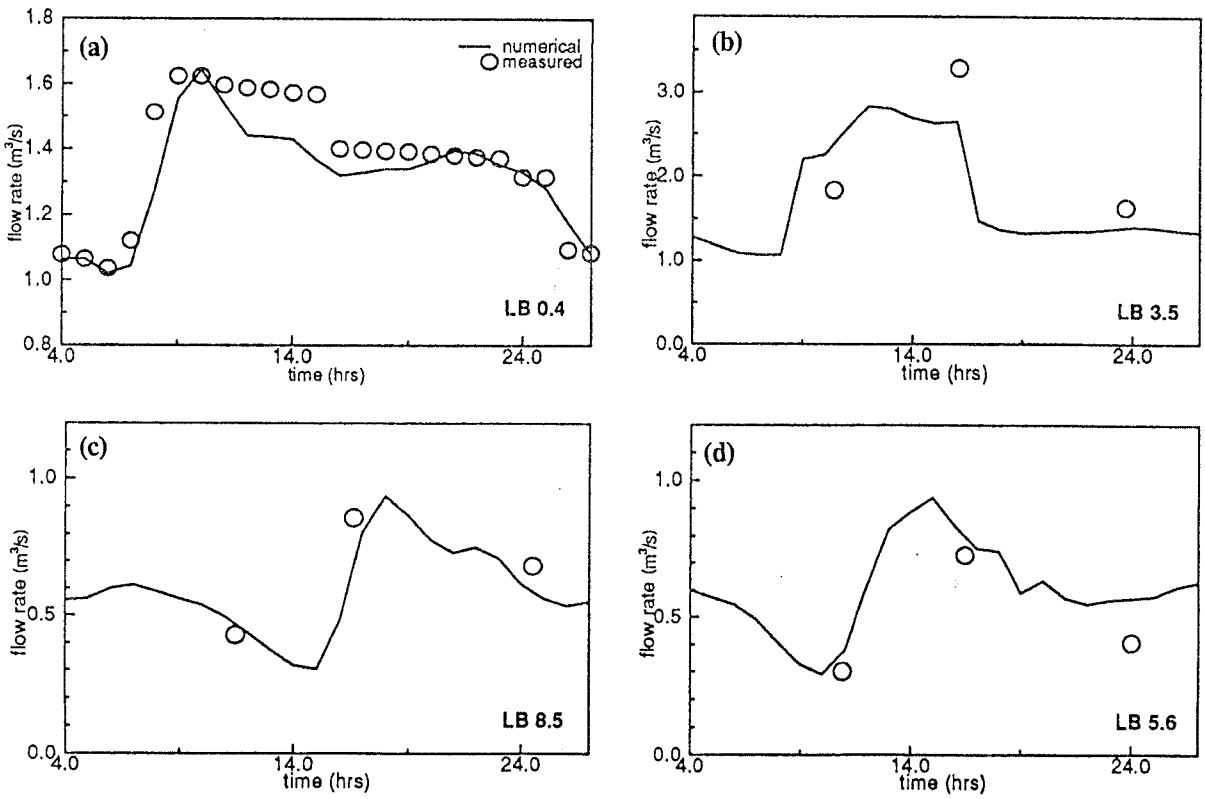

FIG. 4. Flow Rate

Data for Heat Transport Module

The initial temperature distribution in the creek was assumed to vary linearly with the distance between points of observation in a fashion similar to the hydrodynamic module. Table 5 shows the parameters for the heat transport module of Boulder Creek.

Unfortunately, there are no available field measurements for β', η, A_b, and the parameters for the sediments (α, C_s, and ρ_s). Dake and Harleman (1969) recommended that $\beta' = 0.4$ and $\eta = 0.05$ for clear waters after reviewing the measurements of temperature values in several lakes. The value of β' increases when the water system is highly contaminated. It is assumed that the sediment material is composed of stone throughout the entire creek length. The penetration depth of heat into the sediments is about 0.25 m for the diurnal case (Kim 1993; Jobson 1977). To consider no temperature variation at the deep sediment depth, the value of 0.6 m is selected.

Sensitivity tests of C_d and A_b were performed in Boulder Creek. The values of calculated water temperatures with different C_d and A_b are compared to each other at three different times (8 a.m., noon, and 5 p.m.) and four different locations (LB 0.4, LB 3.5, LB 5.6, and LB 8.5). Two cases with C_d = 250 and 500 and $A_b = 0.5$ and 0.95 are selected. It is revealed that the relative variations or errors are bounded within approximately 3 and 15%, respectively. These tests show that the water temperature decreases as the dispersion constant increases or the albedo decreases.

Meteorologic data which include air temperature, dew-point temperature, wind speed, radiation, and precipitation with a 5-min time base were obtained from the National Weather Service (MESONET data). Three MESONET stations are close to the Boulder Creek study area. The Longmont station's meteorologic data was used after considering the site's altitude and characteristics. Fig. 5 shows the Longmont data.

Inflow and WWTP effluent temperatures are regressed with sinusoidal functions to estimate intermediate values between measured data points. The shading factor of incoming shortwave solar radiation by trees and other objects is negligible in Boulder Creek and becomes zero. There is no available temperature data for the Vermont Reservoir effluent. So, the values of LB-0.1 are used as an alternative for the unknown Vermont Reservoir temperature.

TABLE 5. Parameters for Heat Transport Module

Parameter (1)	Value (2)
Sediment depth L_2 (m)	0.6
Space step for sediment zone Δz (m)	0.06
Time step Δt (s)	120
Thermal diffusivity α (m^2s^{-1})—stone	0.0000009
Specific heat C_s ($J\ kg^{-1}\ °C^{-1}$)—stone	799.8
Density ρ_s ($kg\ m^{-3}$)—stone	2,500
Albedo of bed material A_b	0.95
Fraction of solar radiation absorbed at surface water β'	0.4
Extinction coefficient η (m^{-1})	0.05
Coefficient related to air temperature in H_aA'	0.7
Rainfall rate (ms^{-1}) I	0
Dispersion constant C_d	250

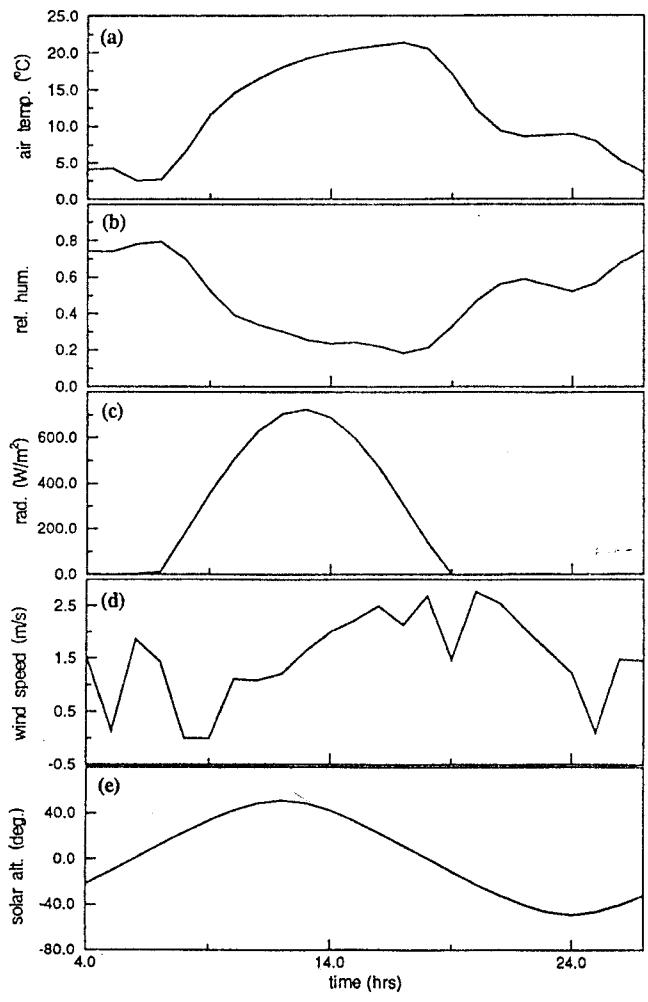

FIG. 5. Longmont Data for Boulder Creek Temperature Simulation

Simulation Results

This module was run for two days in the same manner as the hydrodynamic module. Fig. 6 shows the measured and calculated values of water temperature at each sampling site. The diurnal trend of temperature variation is affected by the assumed sediment material. Generally, the temperature values of stone are lower than those of sand in the daytime, when the water temperature is higher than the sediment temperature, and vice versa at night, because the higher thermal diffusivity of stone tends to enhance the heat conduction. Also, these graphs indicate that sediment interaction affects water temperature and the type of sediment material appears to have an effect on the temperature response characteristics of the Boulder Creek water system.

To quantify the goodness of the results, Fig. 7, which is for a calculated temperature versus a measured temperature, is developed. The standard error of the calculated values $S_{c/m}$ quantifies the spread around the measured values. This error can be determined as

$$S_{c/m} = \sqrt{\frac{S_r}{N-2}} \tag{36}$$

where S_r = sum of the squares of the residuals (the difference of calculated and measured values); and N = number of data points. The sum of the squares of the residuals is 22.2 and the standard error becomes 1.0. If the three points that are far away from the linear line are removed in this process, the standard error becomes 0.56. It is concluded that the standard error of the calculation values is small.

Another sensitivity test was conducted to assess the effect of energy flux at the sediment-water interface. In a fashion similar to the tests of C_d and A_b, three different times and four different locations are selected. The results are compared with the reference values—without considering sediment material. As shown in Fig. 8, the relative errors are bounded within approximately 8%.

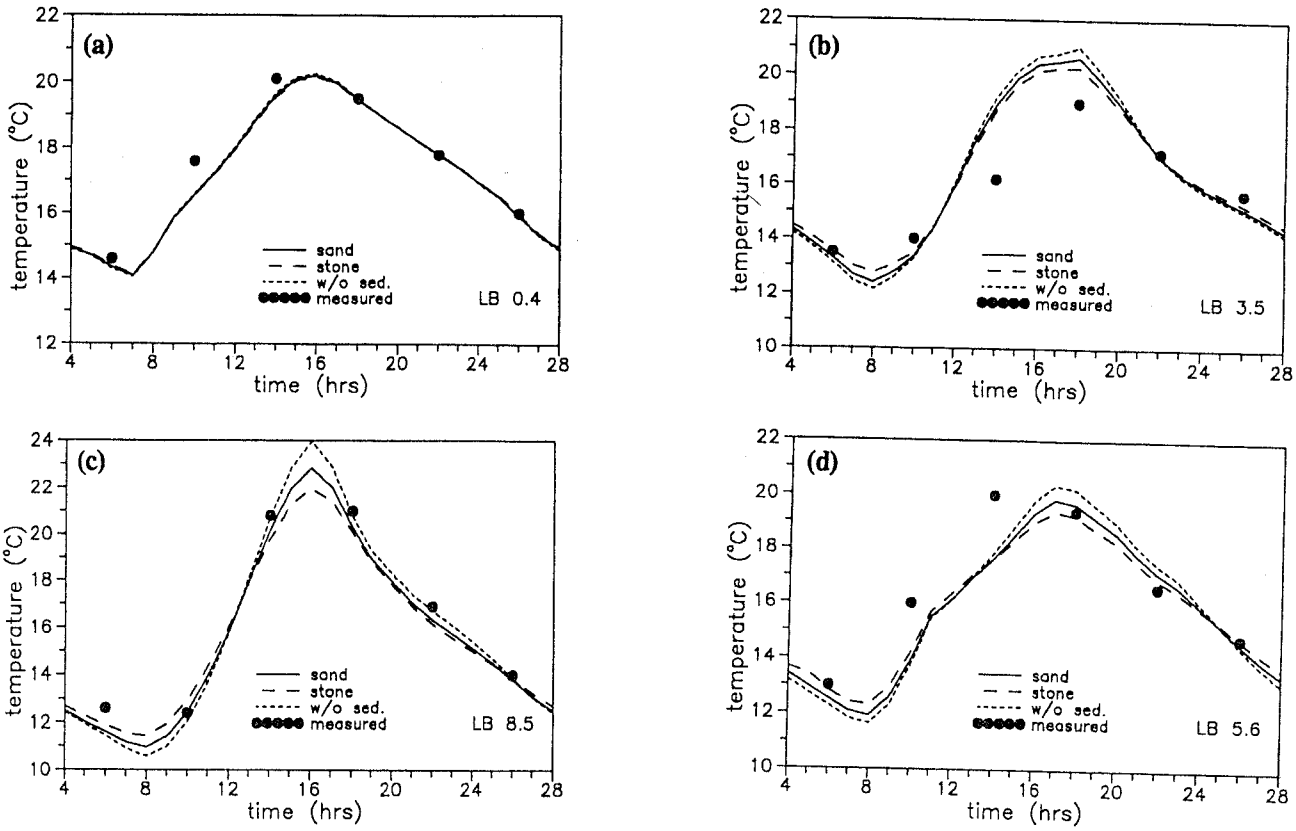

FIG. 6. Water Temperature

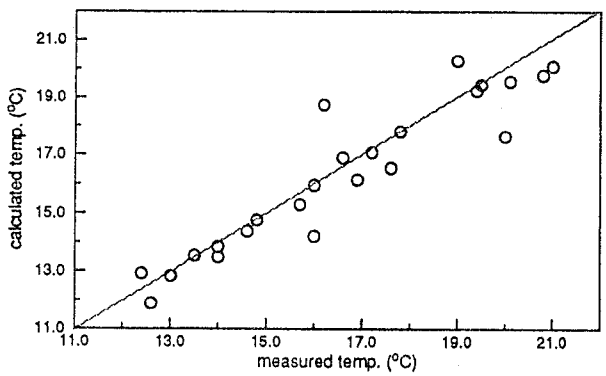

FIG. 7. Correlation between Measured and Calculated Values

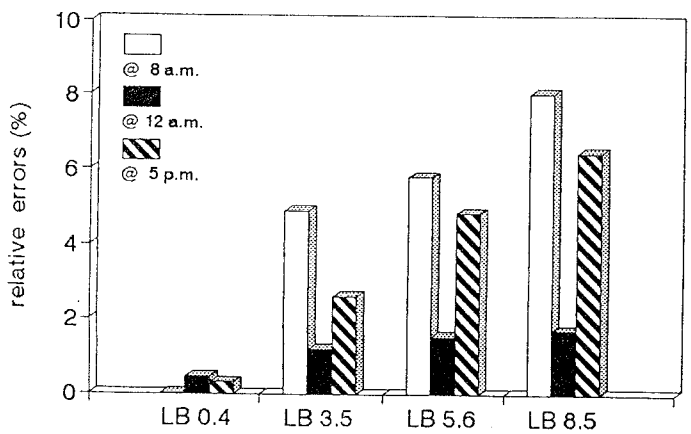

FIG. 8. Sensitivity Tests with and without Sediment

The results reveal the general trend of temperature variation in Boulder Creek, specifically the peak temperature at each sampling site. It is very important to know the peak temperature and peak time of a given environmental system, because elevated water temperatures affect the aquatic ecosystem directly or indirectly.

CONCLUSIONS

The model presented is capable of simulating one-dimensional heat transport in highly transient, shallow, and clear water systems. Simulated temperatures are compared with values measured in the field. A field application of this model indicates that the model effectively simulates heat transport. But a large data set is needed to run this model precisely. The running of the model with another data set for verification will enhance its application in real fields.

The development of the hydrodynamic and heat transport modules will provide a general framework for the simulation of chemical or biological constituents in highly transient water systems. The model application increases our understanding of heat transport including the effects of bottom sediments. Several features, such as the following, are important:

1. Coupling water and sediment. The heat transport module is based on the coupling of transport in surface water systems and diffusion in the sediment zone. The flux of heat energy at the sediment-water interface couples the equations. The governing equations differ from the conventional heat transport equations, which do not consider the net solar radiation available for direct warming of the channel bed and heat flux at the sediment-water interface.
2. Simulation. To implement this approach, a fully implicit finite difference method is used. Application of this

model in Boulder Creek revealed that water temperatures are affected by sediment interaction and the type of sediment material. The higher thermal diffusivity tends to enhance the heat conduction.

3. Hydrodynamic representations. To provide a flexible modeling framework, the resultant model is capable of simulating heat transport under both dynamic and kinematic flow systems.

Our model ignores pool-riffle sequences in the small creek bed. The deep pools are sometimes thermally stratified, with relatively little mixing between the surface flow and the deeper body of water. The assumption of a one-dimensional bed conduction model would be invalid in a water body of high temperature gradient along the creek length. Such effects are beyond the scope of this paper but could be addressed in future research.

APPENDIX I. REFERENCES

Amein, M., and Chu, H. L. (1975). "Implicit numerical modeling of unsteady flows." *J. Hydr. Div.*, ASCE, 101(6), 717–731.

Babajimopoulos, C., and Papadopoulos, F. (1986). "Mathematical prediction of thermal stratification of Lake Ostrovo (Vegoritis), Greece." *Water Resour. Res.*, 22(11), 1590–1596.

Bowie, G. L. et al. (1985). "Rates, constants, and kinetics formulation in surface water quality modeling." *2nd Ed., Rep. EPA 600/3-85/040*, U.S. Envir. Protection Agency, Athens, Ga.

Brown, L. C., and Barnwell Jr., T. O. (1987). "The enhanced stream water quality models QUAL2E and QUAL2E-UNCAS: documentation and user model." *Rep. EPA/600/3-87/007*, U.S. Envir. Protection Agency, Athens, Ga.

Chapra, S. C., and Canale, R. P. (1988). *Numerical methods for engineers*, 2nd Ed., McGraw-Hill Book Co., Inc., New York, N.Y.

Chen, Y. H., and Simons, D. B. (1975). "Mathematical modeling of alluvial channels." *Proc., ASCE Symp. on Modelling Techniques 'Modeling 75,'* Vol. 1, ASCE, New York, N.Y.

Cunge, J. A., Holly, F. M., and Verwey Jr., A. (1980). *Practical aspects of computational river hydraulics*. Pitman Publishing Ltd., London, England.

Dake, J. M. K., and Harleman, D. R. F. (1969). "Thermal stratification in lakes: analytical and laboratory studies." *Water Resour. Res.*, 5(2), 484–495.

Eagleson, P. S. (1970). *Dynamic hydrology*. McGraw-Hill Book Co., Inc., New York, N.Y.

Edinger, J. E., Brady, D. K., and Geyer, J. C. (1974). "Heat exchange and transport in the environment." *Rep. No. EA-74-049-00-3*, Electric Power Res. Inst. Publ., Palo Alto, Calif.

Fischer, H. B., List, E. J., Koh, R. C. Y., Imberger, J., and Brooks, N. H. (1979). *Mixing in inland and coastal waters*. Academic Press, New York, N.Y.

Gromiec, M. J., Loucks, D. P., and Orlob, G. T. (1983). "Stream quality modeling." *Mathematical modeling of water quality: streams, lakes, and reservoirs*. G. T. Orlob, ed., John Wiley & Sons, Inc., New York, N.Y.

Hauser, G. E. (1991). "User's manual for one-dimensional, unsteady flow and water quality modeling in river system with dynamic tributaries." *Rep. No. WR28-3-590-135*, Tennessee Valley Authority, Norris, Tenn.

Hoffman, J. D. (1992). *Numerical methods for engineers and scientists*. McGraw-Hill Book Co., Inc., New York, N.Y.

Jobson, H. E. (1975). "Canal evaporation determined by thermal modeling." *Proc., ASCE Symp. on Modelling Techniques 'Modelling 75,'* Vol. 1, ASCE, New York, N.Y.

Jobson, H. E. (1977). "Bed conduction computation for thermal models." *J. Hydr. Div.*, ASCE, 103(10), 1213–1217.

Jobson, H. E. (1980). "Thermal modeling of flow in the San Diego Aqueduct, California, and its relation to evaporation." *Profl. Paper 1122*, U.S. Geological Survey, Washington, D.C.

Jobson, H. E., and Keefer, T. N. (1979). "Modeling highly transient flow, mass, and heat transport in the Chattahoochee River near Atlanta, Georgia." *Profl. Paper 1136*, U.S. Geological Survey, Washington, D.C.

Kim, K. S. (1993). "Development, application and analysis of the physical aspects of a water-quality modeling framework for highly transient streams," PhD thesis, Univ. of Colorado, Boulder, Colo.

Lai, C. (1986). "Numerical modeling of unsteady open-channel flow." *Advances in hydroscience*, B. C. Yen, ed., Vol. 14, Academic Press, Inc., Orlando, Fla.

Liggett, J. A., and Cunge, J. A. (1975). *Numerical methods of solution of the unsteady flow equations, in unsteady flow in open channels*. Water Resour. Publ., Fort Collins, Colo.

Lyn, D. A., and Goodwin, P. (1987). "Stability of a general Preissmann scheme." *J. Hydr. Engrg.*, ASCE, 113(1), 13–27.

Neumann, G., and Pierson, W. J. (1966). *Principles of physical oceanography*. Prentice-Hall, Inc., Englewood Cliffs, N.J.

Thomann, R. V., and Mueller, J. A. (1987). *Principles of surface water quality modeling and control*. Harper and Rowe, New York, N.Y.

Windell, J. T., Rink, L. P., and Knud-Hansen, C. F. (1988). "A 24-hour synoptic water quality study of Boulder Creek between the 75th Street wastewater treatment plant and Coal Creek." Aquatic and Wetlands Consultants, Inc., Boulder, Colo.

APPENDIX II. NOTATION

The following symbols are used in this paper:

A = area of flow cross section (m^2);
$\mathbf{A}$ = coefficient matrix;
A' = coefficient related to air temperature;
A_b = albedo of bed material;
a = amplitude;
b = stream width (m);
C_d = dispersion constant;
C_w = specific heat of water (J kg^{-1} $°C^{-1}$);
C_s = specific heat of sediment (J kg^{-1} $°C^{-1}$);
c_1 = Bowen's coefficient (kg $m^{-1}s^{-2}$ $°C^{-1}$);
D = longitudinal dispersion coefficient (m^2s^{-1});
e_a = air-vapor pressure (kg $m^{-1}s^{-2}$);
e_{sat} = saturated vapor pressure (kg $m^{-1}s^{-2}$);
g = acceleration due to gravity (ms^{-2});
H_a = long-wave atmospheric radiation (J $m^{-2}s^{-1}$);
H_{ar} = reflected long-wave atmospheric radiation (J $m^{-2}s^{-1}$);
H_B = flux of thermal energy due to temperature differential between the water and bed (J $m^{-2}s^{-1}$);
H_{br} = long-wave radiation from water (J $m^{-2}s^{-1}$);
H_c = conductive heat transfer (J $m^{-2}s^{-1}$);
H_e = evaporative heat transfer (J $m^{-2}s^{-1}$);
H_{nsr} = net solar radiation available for warming channel bed (J $m^{-2}s^{-1}$);
H_R = rain falling heat transfer (J $m^{-2}s^{-1}$);
H_s = shortwave solar radiation (J $m^{-2}s^{-1}$);
H_{sr} = reflected shortwave solar radiation (J $m^{-2}s^{-1}$);
H_T = surface flux of thermal energy (J $m^{-2}s^{-1}$);
h = depth of flow (m);
I = rainfall rate (ms^{-1});
K = conveyance factor;
k = thermal conductivity (J $m^{-1}s^{-1}$ $°C^{-1}$);
L_2 = sediment depth (m);
N = number of data points;
NX = computational segments;
NZ = number of segments into the sediment;
n = Manning's coefficient;
p = wetted perimeter of the channel (m);
Q = flow rate (m^3s^{-1});
q = lateral inflow (m^2s^{-1});
R = hydraulic radius (m);
$\mathbf{R}$ = forcing function vector aggregating the known values;
R' = relative humidity;
r = correlation coefficient;
$S_{e/m}$ = standard error;
S_f = energy slope;
S_r = sum of the squares of the residuals;
S_0 = channel bottom slope;
T = cross-sectional average water temperature (°C);
T_a = air temperature (°C);
T_d = dew-point temperature (°C);
T_L = water temperature in lateral inflow (°C);
T_m = mean water temperature (°C);
T_s = sediment temperature (°C);
T_w = wet-bulb air temperature (°C);
t = time (s);

U_w = wind speed measured at a height of 7 m above the water (ms^{-1});
u = mean velocity (ms^{-1});
u' = x-component average velocity of lateral inflows q (ms^{-1});
u_* = shear velocity (ms^{-1});
w = top width of the channel (m);
$\mathbf{X}$ = vector representing the unknown variables;
x = distance along the stream (m);
z = bed elevation (m);
α = thermal diffusivity of the sediment (m^2s^{-1});
β = momentum correction factor;
β' = fraction of solar radiation absorbed at the surface water;
$\tilde{\beta}$ = solar altitude (degree);
Δt = step of time (s);
Δx = step of space (m);
Δz = step of space into sediment (m);
ε = emissivity of water;
η = extinction coefficients (m^{-1});
θ = weighting factor;
ρ_s = density of sediment (kg m^{-3});
ρ_w = density of water (kg m^{-3});
σ = Stefan-Boltzmann constant (J $m^{-2}s^{-1}$ $°K^{-4}$); and
ω = angular frequency (rad s^{-1}).

Subscripts

j = space line.

Superscripts

n = time line.